Magnetic field control of the Franck-Condon coupling of few-electron quantum states

Supplementary Material

P. L. Stiller, A. Dirnaichner, D. R. Schmid, and A. K. Hüttel*
Institute for Experimental and Applied Physics, University of Regensburg, 93040 Regensburg, Germany
(Dated: December 6, 2018)

CONTENTS

I. HARMONICITY AND EXCITATION ENERGY

Figure S1(a) shows a schematic trace $\mathrm{d}I/\mathrm{d}V_{\mathrm{sd}}(V_{\mathrm{sd}})$ for constant B and V_{g}. From such traces, the peak distances ΔV_{sd1}, ΔV_{sd2}, ΔV_{sd3} as indicated in the drawing can be extracted. They correspond to excitation energies $\Delta\varepsilon_1$, $\Delta\varepsilon_2$, $\Delta\varepsilon_3$. The conversion from bias voltage to energy is based on the capacitances in the quantum dot system and can be illustrated by the sketch of Fig. S1(b). Given the slopes $\Delta V_{\mathrm{sd}}/\Delta V_{\mathrm{g}}$ of the two edges of the single electron tunneling region in the stability diagram, $s_1 < 0$ and $s_2 > 0$,

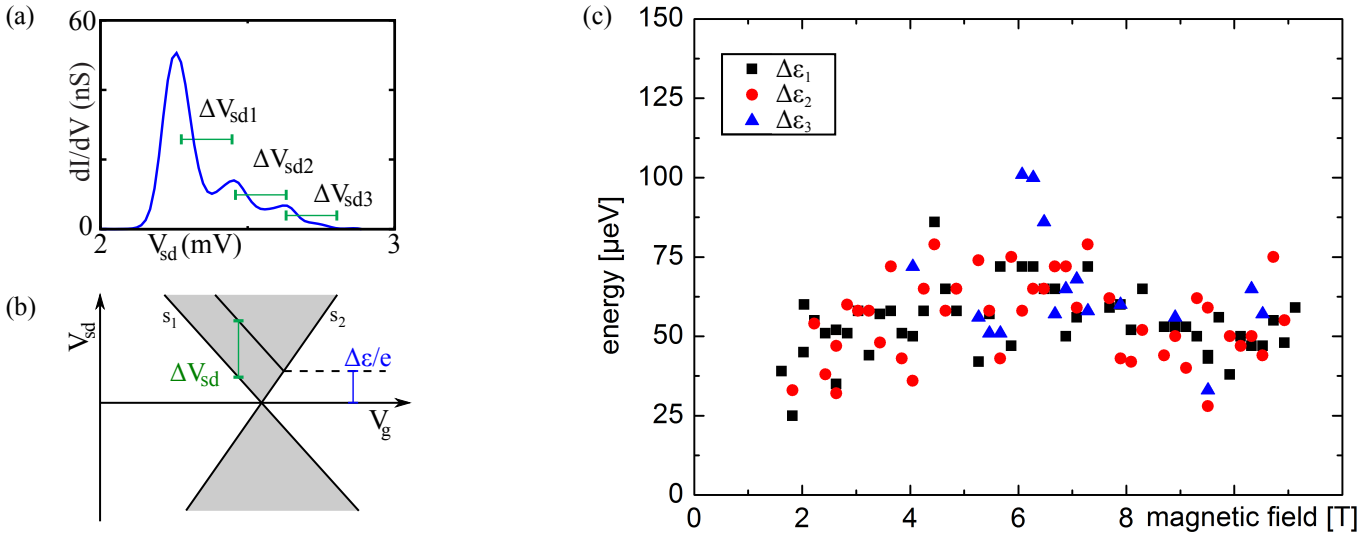

Supplementary Figure S1. (a) Example trace $\mathrm{d}I/\mathrm{d}V_{\mathrm{sd}}(V_{\mathrm{sd}})$ for constant B and V_{g}. For each such trace, the distances ΔV_{sd} between main peak and first side peak, first side peak and second side peak, and second side peak and third side peak are extracted where possible. (b) Using the slopes $\Delta V_{\mathrm{sd}}/\Delta V_{\mathrm{g}}$ of the two edges of the single electron tunneling region in the stability diagram, $s_1 < 0$ and $s_2 > 0$, the bias differences ΔV_{sd} can be converted to energy differences $\Delta\varepsilon$. (c) Resulting excitation energies $\Delta\varepsilon_1$, $\Delta\varepsilon_2$, $\Delta\varepsilon_3$ corresponding to the distances ΔV_{sd1}, ΔV_{sd2}, ΔV_{sd3}, as extracted from the data of Fig. 2(b) of the main text.

* andreas.huettel@ur.de

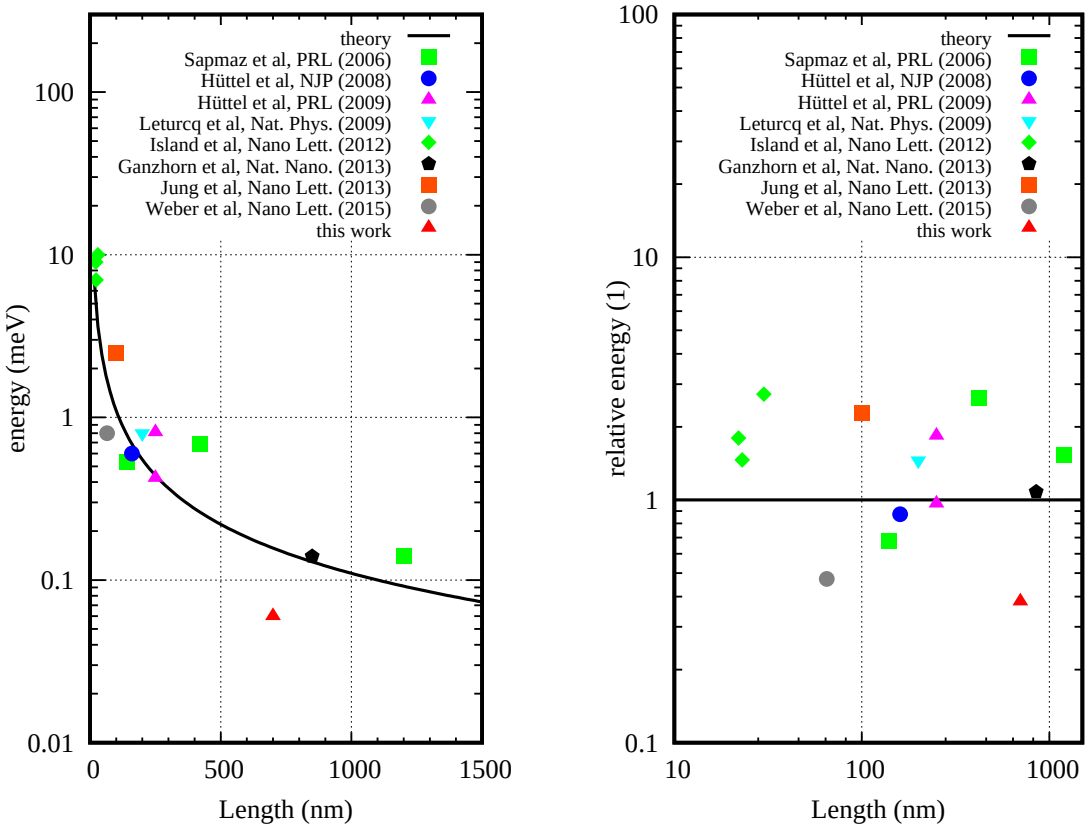

Supplementary Figure S2. Overview of carbon nanotube longitudinal vibration oscillator quanta $\Delta\varepsilon = \hbar\omega$ observed in published literature [1–8], as function of device length, in comparison with the theoretical result $\Delta\varepsilon_{\rm th}(L) = 110\,{\rm meV}/L[{\rm nm}]$. Left: unscaled $\Delta\varepsilon(L)$, linear length scale; right: $\Delta\varepsilon(L)/\Delta\varepsilon_{\rm th}(L)$, logarithmic length scale.

as indicated in Fig. **S1**(b), the conversion can be derived from elementary geometry as

$$\Delta\varepsilon = \frac{1}{e}\,\frac{1}{1-\frac{s_1}{s_2}}\,\Delta V_{\rm sd}. \tag{S1}$$

The result of an evaluation of the data of Fig. 2(b) of the main text is shown in Fig. **S1**(c). Here, the black squares correspond to the excitation energy of the first sideband relative to the base electronic state, the red dots to the one of the second sideband relative to the first sideband, and the blue triangles to the one of the third sideband relative to the second sideband. Within the scatter originating in noise of the current measurement, no clear dependence on the magnetic field is visible, and the sidebands display equal behaviour. This indicates equidistant quantum states of a harmonic oscillator, with a field-independent excitation energy of $\Delta E \simeq 60\,\mu$eV.

The theoretical value for the energy quantum of the carbon nanotube longitudinal vibration is given by [1]

$$\Delta\varepsilon_{\rm th} = \frac{h}{L}\sqrt{\frac{Y}{\rho}}, \tag{S2}$$

where L is the nanotube length, Y is Young's modulus, and ρ is the nanotube mass density. Assuming $\rho = 1.3\,{\rm g/cm^3}$ and $Y = 1\,{\rm TPa}$, this results in [1]

$$\Delta\varepsilon_{\rm th} \approx \frac{0.11\,{\rm meV}}{L(\mu{\rm m})} \tag{S3}$$

For our device with $L = 0.7\,\mu$m, we obtain $\Delta\varepsilon_{\rm th} \simeq 160\,\mu{\rm eV} \simeq 2.7\Delta\varepsilon$. While there is a clear deviation, our measurement still lies within the typical scatter of oscillator quanta observed in experimental literature, see Fig. **S2**.

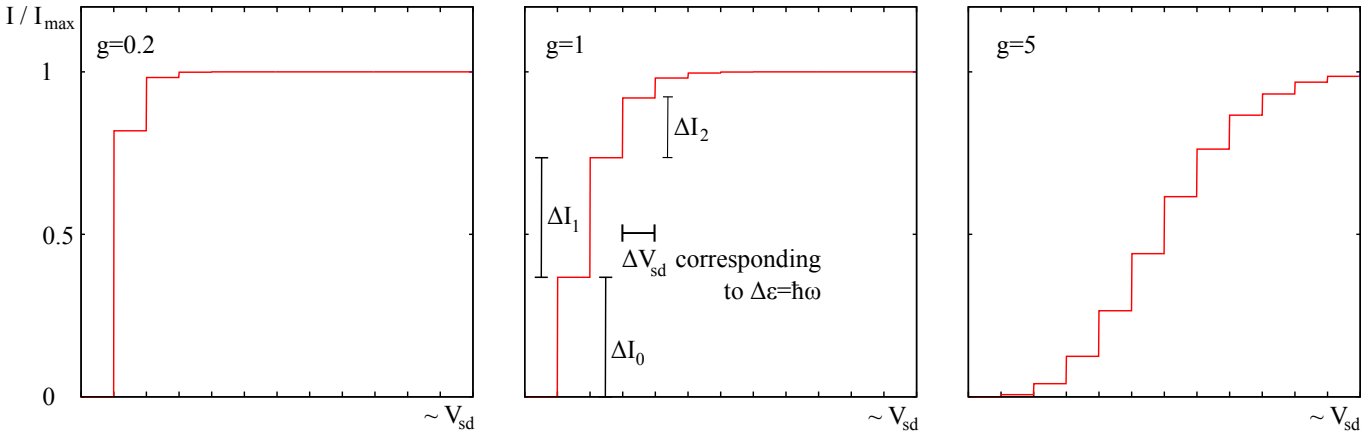

Supplementary Figure S3. Impact of the Franck-Condon coupling parameter g on the SET current $I(V_{\mathrm{sd}})$.

II. g EVALUATION METHODS

The Franck-Condon coupling parameter g describes in the context of single electron tunneling through a carbon nanotube the spatial shift of the nanotube equilibrium position as harmonic oscillator when an additional charge is added to it. It is defined as

$$g = \frac{1}{2}\left(\frac{\Delta x_0}{x_{\mathrm{zpf}}}\right)^2, \tag{S4}$$

where Δx_0 is the shift in equilibrium position due to electrostatic forces when adding an electron to the nanotube,

$$\Delta x_0 = x_0(N+1) - x_0(N). \tag{S5}$$

In the denominator,

$$x_{\mathrm{zpf}} = \sqrt{\frac{\hbar}{m\omega}} \tag{S6}$$

is the characteristic length scale of the harmonic oscillator, describing the wave function extension of the ground state and/or its zero point fluctuations. For $\hbar\omega = 60\,\mu$eV and $m = 1.3\times10^{-21}$ kg [9], we obtain $x_{\mathrm{zpf}} = 0.9$ pm.

At finite temperature, a harmonic oscillator can both absorb and emit vibrons. Here, in the limit of low temperature and fast vibrational relaxation compared to the tunnel rates, we assume that for any single electron tunneling process we start out in the N electron vibrational ground state. The overlap $|\langle\Psi_0(N)\,|\,\Psi_n(N+1)\rangle|^2$ of the N electron vibrational ground state with a $N+1$ electron state of n vibration quanta increases with n. This leads to a series of equidistant steps in current $I(V_{\mathrm{sd}})$ or peaks in differential conductance $\mathrm{d}I/\mathrm{d}V_{\mathrm{sd}}(V_{\mathrm{sd}})$, whenever sufficient energy for reaching the next vibrational state becomes available.

The contributions of the vibrational states and thus the current step or conductance peak heights are given by the Poisson formula [10, 11],

$$\Delta I_n \propto \frac{e^{-g}g^n}{n!}, \quad n = 0,1,2,\ldots \tag{S7}$$

at an energy $n\hbar\omega$ from the bare electronic state transition. The resulting step function of the current in absence of thermal or lifetime broadening is sketched in Fig. **S3** for different values of g.

Using Eq. (S7), the values of $g(B)$ plotted in Fig. 2(d) of the main text have been obtained using three different but closely related evaluation methods:

- method 1: manually adapt a step function to the current $I(V_{\mathrm{sd}})$
  Since the current decreases again far away from the electronic base line, see the negative differential conductance in Fig. 2(b) of the main text, we use the maximally achieved value in the vicinity of one electronic base line as theoretical maximum current.

- method 2a: calculate the area below the differential conductance peaks $\mathrm{d}I/\mathrm{d}V_{\mathrm{sd}}(V_{\mathrm{sd}})$ of the electronic ground state transition A_0 and the first vibrational side band A_1 and use

$$\frac{A_1}{A_0} = \frac{\Delta I_1}{\Delta I_0} = \frac{\frac{e^{-g}g^1}{1!}}{\frac{e^{-g}g^0}{0!}} = g \tag{S8}$$

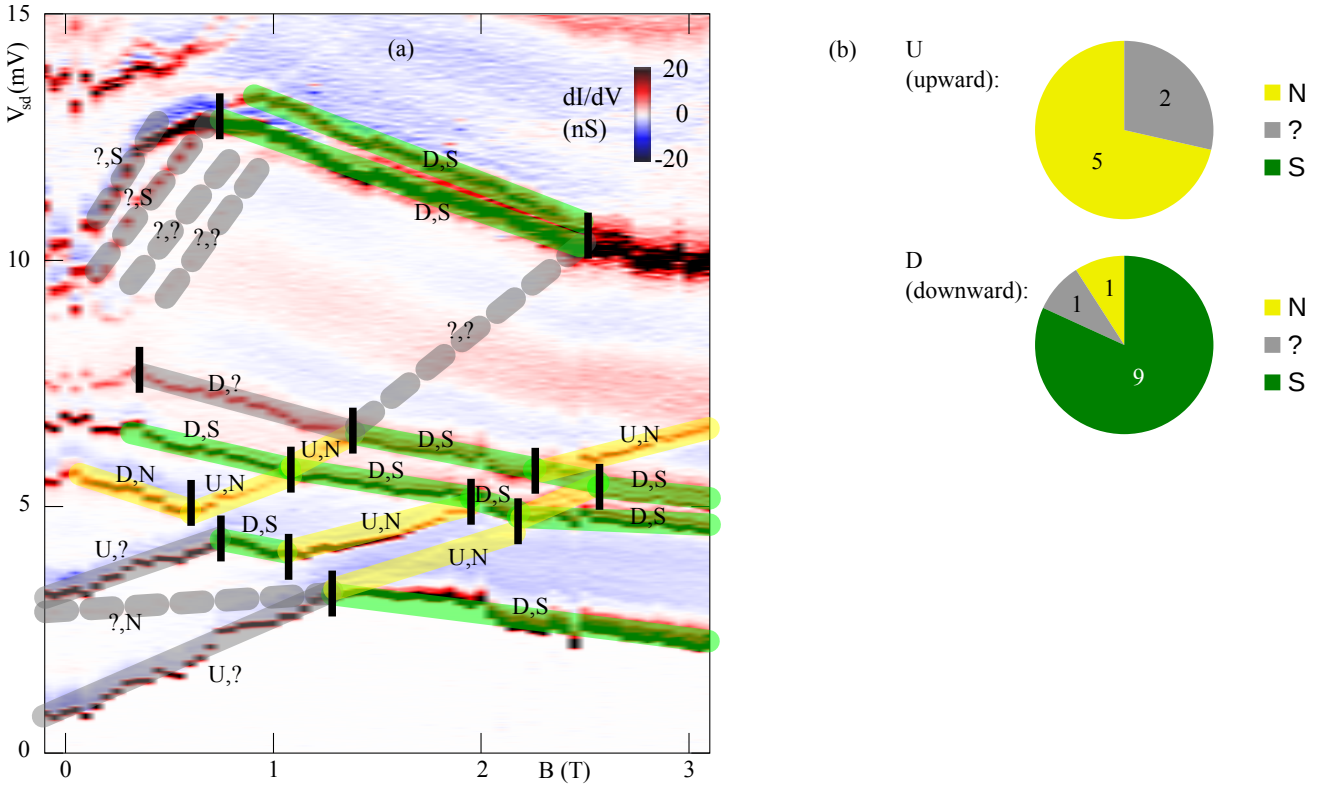

Supplementary Figure S4. (a) Larger version of Fig. 3(a) of the main text, with all conductance lines marked which have been checked for harmonic side bands. "U" and "D" correspond to the characteristic upward and downward slope of a single electron orbital magnetic moment $\pm\mu_{\rm orb}$; "S" indicates the presence, "N" the absence of harmonic side bands. (b) Pie diagrams indicating the occurrence of side bands on upsloping and downsloping lines.

- method 2b: proceed as in 2a, but use the first and second vibrational side band, with the relation

$$\frac{A_2}{A_1} = \frac{\Delta I_2}{\Delta I_1} = \frac{g}{2} \tag{S9}$$

As can be seen in Fig. 2(d) of the main text, the three methods agree well within the error bars. In particular the agreement between evaluation methods 2a and 2b also confirms the Franck-Condon behaviour of the system.

III. SYSTEMATIC EVALUATION OF THE EXCITATION SPECTRUM

The background plot of Fig. S4(a) is a larger version of Fig. 3(a) in the main text. Here, the black vertical bars indicate how the observed conductance lines have been divided into segments; the segments have been classified according to their approximate slope as "U", "D" (with addition of one electron orbital magnetic moment) or "?" otherwise. Each line segment has been checked for harmonic side bands. Where these have clearly been found, this is indicated by "S", where not, by "N". Due to the noise level in the data, the decision is not always possible, then leading to a "?" designation.

The pie diagrams of Fig. S4(b) summarize the result. For "U"-lines, in most cases side bands are clearly absent, while they are almost always present for "D"-lines. The observation that $g(B)$ decreases for decreasing magnetic field (see Fig. 3(f) of the main text) can explain the occurrence of a "D,N" classification at $B \leq 0.5\,\mathrm{T}$ and $V_{\rm sd} \sim 5\,\mathrm{mV}$; at very low values of g the side bands will disappear in the noise background.

[1] S. Sapmaz, P. Jarillo-Herrero, Ya. M. Blanter, C. Dekker, and H. S. J. van der Zant, "Tunneling in suspended carbon nanotubes assisted by longitudinal phonons," Phys. Rev. Lett. **96**, 026801 (2006).

[2] A. K. Hüttel, M. Poot, B. Witkamp, and H. S. J. van der Zant, "Nanoelectromechanics of suspended carbon nanotubes," New Journal of Physics **10**, 095003 (2008).

[3] A. K. Hüttel, B. Witkamp, M. Leijnse, M. R. Wegewijs, and H. S. J. van der Zant, "Pumping of vibrational excitations in the Coulomb-blockade regime in a suspended carbon nanotube," Phys. Rev. Lett. **102**, 225501 (2009).

[4] R. Leturcq, C. Stampfer, K. Inderbitzin, L. Durrer, C. Hierold, E. Mariani, M. G. Schultz, F. von Oppen, and K. Ensslin, "Franck-Condon blockade in suspended carbon nanotube quantum dots," Nature Physics **5**, 327 (2009).

[5] J. O. Island, V. Tayari, A. C. McRae, and A. R. Champagne, "Few-hundred GHz carbon nanotube nanoelectromechanical systems (NEMS)," Nano Letters **12**, 4564 (2012).

[6] M. Ganzhorn, S. Klyatskaya, M. Ruben, and W. Wernsdorfer, "Strong spin–phonon coupling between a single-molecule magnet and a carbon nanotube nanoelectromechanical system," Nature Nanotechnology **8**, 165 (2013).

[7] M. Jung, J. Schindele, S. Nau, M. Weiss, A. Baumgartner, and C. Schnenberger, "Ultraclean single, double, and triple carbon nanotube quantum dots with recessed Re bottom gates," Nano Letters **13**, 4522 (2013).

[8] P. Weber, H. L. Calvo, J. Bohle, K. Goß, C. Meyer, M. R. Wegewijs, and C. Stampfer, "Switchable coupling of vibrations to two-electron carbon-nanotube quantum dot states," Nano Letters **15**, 4417 (2015).

[9] D. R. Schmid, P. L. Stiller, C. Strunk, and A. K. Hüttel, "Magnetic damping of a carbon nanotube nano-electromechanical resonator," New Journal of Physics **14**, 083024 (2012).

[10] S. Braig and K. Flensberg, "Vibrational sidebands and dissipative tunneling in molecular transistors," Phys. Rev. B **68**, 205324 (2003).

[11] J. Koch, F. von Oppen, and A. V. Andreev, "Theory of the Franck-Condon blockade regime," Phys. Rev. B **74**, 205438 (2006).